

Geological features and H-O-S-Pb isotopes of Au (-Sb-W) deposit in south China's Xuefeng arcuate mineralization belt

Xuefeng arcuate mineralization belt is one of the key gold-bearing polymetallic mineralization belts in South China. This paper analyses the sulphide, lead, hydrogen and oxygen isotopes of three typical deposits in the belt. The results show that the $\delta^{34}\text{S}$ values of Bake gold deposit in the south varies significantly but consistently with the sulphide range of the local Banxi Group stratum, indicating that the mineral-bound sulphide came from the local stratum. To the north, the $\delta^{34}\text{S}$ values of Zhazixi Sb-Au deposit have a small range as does the northern-most Woxi Au-Sb-W deposit. In particular, the $\delta^{34}\text{S}$ values of Woxi deposit fall within 2.8‰~-1.5‰, which is consistent with the sulphide content in granite. This means the sulphur mainly originates from magmatite. According to the isotope analysis of hydrogen and oxygen, most of the fluids derived from formation water and meteoric water in the south, and from magmatic water and metamorphic water in the middle and northern parts. Comprehensive analysis of mineralization geology and tectonic evolution leads to the conclusion that the minerals formed in the Early Paleozoic period functioned as the depositional stratum, the mineralization in the Indosinian movements during Jurassic-Cretaceous period was mainly driven by magmatic fluid.

Keywords: Xuefeng belt, isotopes analysis, mineralization, sources.

1. Introduction

Xuefeng arcuate mineralization belt (hereinafter referred to as "Xuefeng belt" or simply "the belt") is one of the key gold-bearing polymetallic mineralization belts

Messrs. Liangliang Jia, Tagen Dai, Chaozhuang Xi and Dexian Zhang, MOE Key Laboratory of Metallogenic Prediction of Nonferrous Metals, School of Geosciences and Info-Physics, Central South University, Changsha 410 083, Liangliang Jia, Hunan Institute of Coal Geological Exploration, Changsha 410 083, Chaozhuang Xi, Geological Survey Institute for Nuclear Resources, Guizhou Geological Exploration Bureau for Nonferrous Metals and Nuclear Industry, Guiyang 550 005, Chaozhuang Xi, Hunan Gold Group Co., Ltd., Changsha 410 083, China and Richard C. Bayless, Department of Natural Sciences, Shawnee State University, Portsmouth, OH, 45662, USA. Corresponding author e-mail: xczcsummmmm@126.com

in South China. In the belt, gold (Au) is the primary mining material, while antimony (Sb) and tungsten (W) are secondary ones. Around 500 primary gold-bearing polymetallic deposits have been recognized in the area, including Woxi Au-Sb-W deposit, Zhazixi Sb-Au deposit, Chanzipping gold deposit, Pingcha gold deposit, Taojinchong gold deposit, Dayetang gold deposit, Bake gold deposit and Banxi antimony deposit. Located in the north of the belt, Woxi Au-Sb-W deposit stands out as the largest deposit.

In the area, gold and other metal minerals are mainly borne in quartz veins, and subject to stratum and tectonic influences. Many scholars have explored the source of mineralization materials/fluids and mineralization epoch in Xuefeng Belt. However, their research was often restricted to provincial-level administration regions, as the belt spans across several provinces, including Hunan, Guizhou and Guangxi. Based on the limited information in each province, scholars have the disagreement on the source of mineralization materials/fluids and mineralization forces among the gold-bearing polymetallic deposits in the belt and most scholars held that the gold-bearing polymetallic deposits share similar sources of mineralization materials and fluids, even though gold is the main mining product only in the southern, middle and northern parts of the belt.

There are still differences on tectonic history, mineralization epochs and elemental compositions of minerals. In the south of the belt lies a visible, low-sulphide gold deposit formed in the early Palaeozoic era [1] (Fig.1). The middle and northern parts of the belt are covered by high-sulphide gold-bearing polymetallic deposits, e.g. Au-Sb, Sb-W and Au-Sb-W, formed in the Indosinian movements during Jurassic-Cretaceous period [1] (Fig.1). In these gold-bearing deposits of the middle and northern parts of the belt, gold mainly exists in the form of particles enclosed by sulphide. Hence, there are clear differences in the source of mineralization materials and fluids among the southern, middle and northern parts of the belt [2,3].

This paper investigates the mineral compositions of three deposits at three typical places in the belt, namely Bake gold

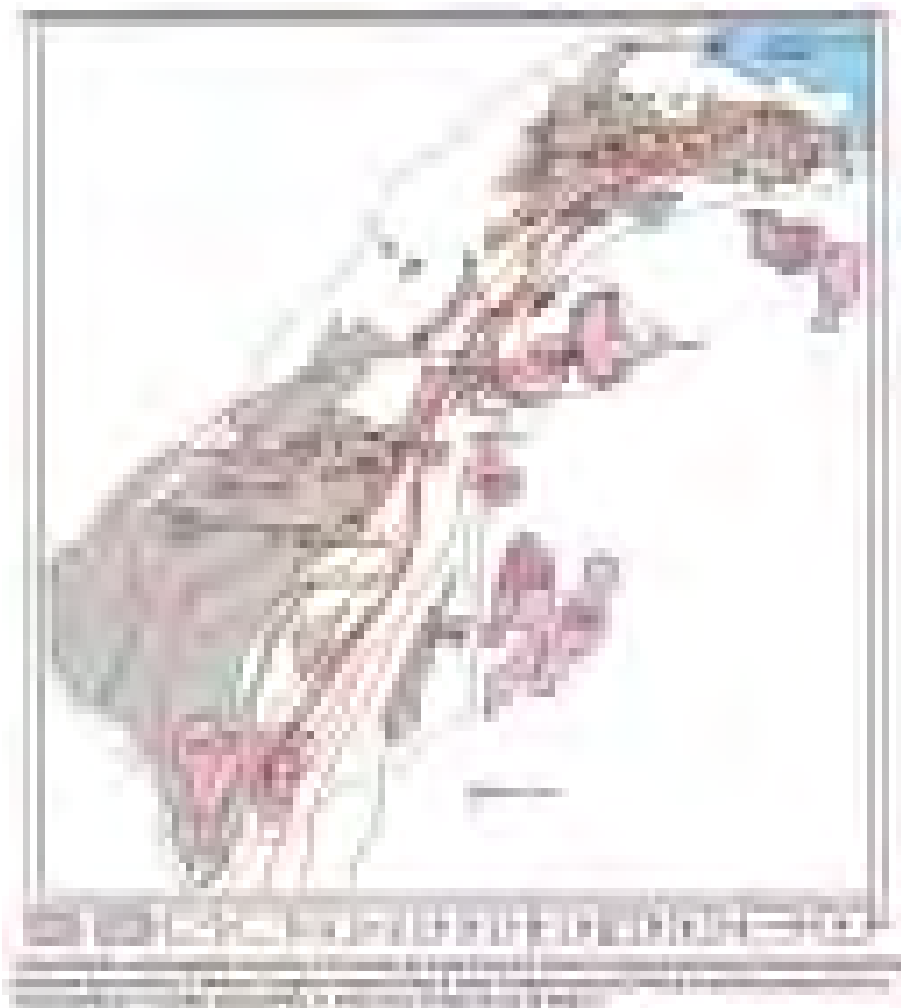


Fig.1 Regional geology map of Xuefeng belt

deposit in the south, Zhazixi Sb-Au deposit in the middle and Woxi Au-Sb-W deposit in the north. Hydrogen (H), oxygen (O), sulphide (S) and lead (Pb) isotopes were examined to reveal the source and evolution of mineralization materials and fluids. This research provides a compelling proof that the mineralization materials and fluids came from different sources in different parts of the belt, and that mineralization in Xuefeng belt occurred in two distinct periods.

2. Regional geological background

The Xuefeng belt is located in the south-east side of the south-west section of South China's land axis. The northeast side of the Xuefeng belt begins on the west edge of Dongting Lake Sunken land while its south-west boundary is found where the fold belt north of Guilin and the Anhua-Xupu-Jingzhou Great Large Fault pass through the Xuefeng belt from south to north and cross two large tectonic units of Yangtze platform areas and South China's fault systems; its north-south side is the Yangtze platform areas while south-east is South China's fault belt; Anhua-Shupu-Jingzhou deep and great large fault was active for a long period of geologic

time and that resulted in remarkable differences across the fault in terms of tectonics and resulting geology (Fig.1).

The raised areas on the western platform of the fault are the main distribution areas of gold-bearing polymetallic deposits in the belt. The most common exposed strata include the widely distributed thick sequences of metamorphic clastic, slate and cinerite of Lengjiayi Group and Banxi Group. These rocks form the basement of Xuefeng belt. The upper strata were formed in Sinian, Cambrian, Carboniferous, Permian, Cretaceous and Tertiary periods, and are dispersed across the upper portion of the deepest base rocks. Some Ordovician residuals are present, but there is a lack of Devonian rock. The upper strata of Carboniferous rocks are scattered as tectonic residuals and erosional placers. In terms of the host strata, Banxi Group stratum is classified as the primary stratum, while Lengjiayi Group and Sinian strata are classified as secondary strata. These strata have uniform occurrence in large, open faulted anticlines.

In Xuefeng belt, the faults are well developed and spread across tens of kilometres in the NE, N-NE, NW and near E-W directions. Two tectonic faults

sometimes intersect to form a rhombus pattern with NE, N-NE, northwest and near E-W orientations. These tectonic structures have controlled the distribution of the gold-bearing polymetallic deposits of the belt (Fig.1). In particular, the eastern edge of Xuefeng belt is dominated by carbonaceous siliceous rocks of Sinian and Cambrian periods. These strata are only partially exposed in an N-NE fault belt, where faults and folds developed under extrusion leave them as cliffs underneath Sinian stratum.

The intermediate-acid magmatite rocks are distributed unevenly in Xuefeng belt, but occurs primarily in an eastern region, in the northern part, and in the Sanfang mountain area and the Yuanbao mountain area north of Guilin. From south-to-north, the emplacement age of granite becomes increasingly younger, with 492Ma in the south to 90Ma in the north (Fig.1). The mineral compositions and deposit age vary from place to place, but still follow a certain trend in the south-north direction. In the south of the belt lies a visible, low-sulphide gold deposit formed in the early Palaeozoic era. The primary gold deposit is situated in the south, which was formed in the early Palaeozoic era, while the Au-Sb, Sb-W and

Au-Sb-W deposits in the middle and northern parts were formed in the Indosinian movements during Jurassic-Cretaceous period.

3. Specific deposit features

3.1 BAKE GOLD DEPOSIT

Bake deposit is located on the axis of Wenjiang anticline, and the southwestern edge of Xuefeng belt in Jinping County, Guizhou Province. With the N-NE trending Wenjiang fault passing right through it, the deposit is 1.24km from the NE-trending Jinping-Huitong fault in the north, 6.48km from the NE-trending Jinping-Jingzhou fault in the south, and 1km from the Tonggu-Ouli fault in the NE.

The only exposed stratum in the region is the Proterozoic Wuqiangxi formation of Banxi Group. Identical to the host strata, the orebody has a lamellar and stratified structure. Mineral alteration mainly consists of silicification, arsenopyritization, pyritization, chloritization and carbonatation. The gold has been mined from gold-bearing quartz veins formed through the circulation of low to moderate temperature thermal fluids.

The only ore mineral is native gold. The gangue mineral is primarily quartz, followed by calcite, sericite and chlorite. There is also frequent occurrence of sulphides pyrite and arsenopyrite, as well as occasional presence of gellenite, sphalerite and stibnite.

3.2 ZHAZIXI SB-AU DEPOSIT

Zhazixi deposit, situated in the middle part of Xuefeng belt, is cut through by a magmatite belt in the NW-trending Shaoyang-Chenzhou strike-slip structure. The location marks a turning point (from NE to near E-W) of the tectonic fault lines.

The exposed strata primarily contain the Banxi Group, Sinian, Cambrian and Devonian rocks, plus some Ordovician, carboniferous and permian rocks. Banxi Group rocks are the main host strata of Sb-Au deposits in the region. The large scale tectonic line is composed of NE-trending faults, a series of duplicated folds with short axes, and secondary fault groups. The secondary faults, often distributed on the side of the NE-trending regional fault, form the main tectonic host structures for Sb orebodies.

The orebodies occur in Wuqiangxi formation of Banxi Group in form of veins and are controlled by fractures. The 50+ recognized ore veins fall into 2 groups: Group A (strike $290^{\circ}\sim 110^{\circ}$, dip NNE) and Group B (strike $330^{\circ}\sim 150^{\circ}$, dip NEE). The ore bodies are enriched at the confluence of Group A and Group B veins. The ore minerals include stibnite, gold and scheelite. The gangue minerals are primarily quartz, with some calcite and a trace of pyrite. The deposits occur as fault and fracture.

3.3 WOXI AU-SB-W DEPOSIT

Woxi deposit is located on the northern edge of Xuefeng belt in Yuanling County, Hunan province. The location marks

a turning point (from N-NE to NE-E) of the gold-bearing polymetallic mineralization belt. The massive Woxi fault passes through the northern part of the area. Fold, fracture, clefts, stratification, foliation and rock cleavage are developed in the region, and the strata of the deposit and its surrounding areas are mainly Proterozoic Wuqiangxi and Madiyi formations of Banxi Group.

Madiyi formation is the host strata and an intermediate-acid magmatite vein occurs in the southwestern part of the deposit. Identical to the host strata, the orebody has a lamellar, stratified structure. The texture and structure of ores are relatively simple. Mineral alteration mainly consists of decolouration, silicification, pyritization, chloritization and illitization. The deposit is essentially a quartz vein filled by high-temperature replacement of Sb, W and Au ores.

The primary ore minerals include native gold, stibnite, scheelite, ferberite and pyrite; the secondary minerals are galenite, sphalerite and chalcopyrite. There is also a few arsenopyrite, antimony and gold. The gangue minerals are primarily quartz (80%), with some calcite, ankerite, chlorite and sericite, and a trace of pyrophyllite, illitite and kaoline.

4. Sample collection and analysis

Typical samples were collected from the mining pits Zhazixi Sb-Au deposit and Bake gold deposit to reflect the main mineralization stages of all the deposits. Except where noted by remarks and quotations, the sample assays were completed at the Analysis and Testing Centre of Beijing Research Institute of Uranium Geology (BRIUG).

The hydrogen and oxygen isotopes were analysed through the following steps. The H_2 was extracted by vacuum thermal decrepitation and zinc reduction; pure O_2 was collected from quartz with the Bromo fluoride (BrF_5) method, and then converted to CO_2 in graphite furnace in a vacuum at $500\sim 680^{\circ}C$ [4]. The hydrogen and oxygen components were examined using an MAT-235 mass spectrometer in the Analysis and Testing Centre of BRIUG.

The sulphide isotopes samples were analysed through the following steps. The Cu_2O was mixed as an oxidizer with simple sulphide minerals to produce SO_2 [5]. The product was then frozen and collected, and analysed using an MAT-251 mass spectrometer (precision: $\pm 0.2\%$). The results were evaluated against the Vienna-Canyon Diablo Troilite (VCDT) standard. The sulphide components were examined in the Analysis and Testing Centre of BRIUG.

The lead isotopes samples were analysed through the following steps. The samples were dissolved and separated at $20^{\circ}C$ under the relative humidity of 36%. Strontium, rubidium and lead isotopes were determined by an IsoProbe-TTM thermal ionization mass spectrometer; the lead isotope ratios were determined and the results were adjusted by the international standards to less than the error of 2σ . The lead components were examined in the Analysis and Testing Centre of BRIUG.

TABLE 1: SULPHIDE ISOTOPES IN THE THREE DEPOSITS

Deposit	Sample serial no.	Descriptions	Simple mineral	$\delta^{34}\text{S}_{\text{VCDT}}\%$	Data sources
Bake	BK01	Quartz-arsenopyrite-gold ore with pattern of stripes	Arsenopyrite	5	Yu et al., 1997[6]
	BK02	Quartz-arsenopyrite-gold ore with pattern of stripes	Arsenopyrite	1.6	
	BK03	Quartz-arsenopyrite-gold ore with pattern of stripes	Pyrite	8.95	Chen et al., 2015[7]
	BK04	Quartz-arsenopyrite-gold ore with pattern of stripes	Tungstite	2.67	
	BK05	Quartz-arsenopyrite-gold ore with pattern of stripes	Arsenopyrite	1.7	Lai et al., 2010[8]
	BK06	Quartz-arsenopyrite-gold ore with pattern of stripes	Arsenopyrite	4.9	
	BK07	Quartz-arsenopyrite-gold ore with pattern of stripes	Arsenopyrite	6.8	
	BK08	Quartz-arsenopyrite-gold ore with pattern of stripes	Arsenopyrite	6.7	
Zhazixi	ZZX01	Quartz-tungstite-stibnite ore with pattern of strips	Stibnite	2.1	This study
	ZZX02	Quartz-tungstite-stibnite ore with pattern of strips	Stibnite	3.5	
	ZZX03	Quartz-tungstite-stibnite ore with pattern of strips	Stibnite	2.2	
	ZZX04	Stibnite ore with pattern of bulk	Stibnite	0.3	
	ZZX05	Stibnite ore with pattern of bulk	Stibnite	-2.6	
Woxi	WX01	Quartz-tungstite-stibnite ore with pattern of strips	Stibnite	-1.6	Gu et al., 2004[9]
	WX02	Quartz-tungstite-stibnite ore with pattern of strips	Stibnite	-2.5	
	WX03	Quartz-tungstite-stibnite ore with pattern of strips	Stibnite	-2.4	
	WX04	Quartz-tungstite-stibnite ore with pattern of strips	Stibnite	-2.1	
	WX05	Quartz-tungstite-stibnite ore with pattern of strips	Stibnite	-2.4	
	WX06	Quartz-tungstite-stibnite ore with pattern of strips	Stibnite	-2.4	
	WX07	Quartz-tungstite-stibnite ore with pattern of strips	Stibnite	-2.3	
	WX08	Quartz-tungstite-stibnite ore with pattern of strips	Stibnite	-2.2	
	WX09	Quartz-tungstite-stibnite ore with pattern of strips	Stibnite	-2.6	
	WX10	Quartz-tungstite-stibnite ore with pattern of strips	Stibnite	-1.2	
	WX11	Quartz-tungstite-stibnite ore with bulk pattern	Stibnite	-1.5	
	WX12	Quartz-tungstite-stibnite ore with pattern of strips	Stibnite	-1.8	
	WX13	Quartz-tungstite-stibnite ore with pattern of strips	Stibnite	-1.7	
	WX14	Quartz-tungstite-stibnite ore with pattern of strips	Stibnite	-2.1	
	WX15	Quartz-tungstite-stibnite ore with pattern of strips	Stibnite	-2.3	
	WX16	Quartz-tungstite-stibnite ore with pattern of strips	Stibnite	-2.8	
	WX17	Stibnite ore with pattern of bulk	Stibnite	-2.2	
	WX18	Stibnite ore with pattern of bulk	Stibnite	-2.6	

5. Results

5.1 SULPHIDE ISOTOPES

As shown in Table 1, the $\delta^{34}\text{S}\%$ values of Bake gold deposit were positive and fell within 1.6‰~8.95‰, with an average value of 4.79‰; the $\delta^{34}\text{S}\%$ values of Zhazixi Sb-Au deposit fluctuated around 0‰ and fell within -2.6‰~3.5‰, with an average value of 1.1‰; the $\delta^{34}\text{S}\%$ values of Woxi Au-Sb-W deposit were negative and fell within -2.8‰~-1.5‰, with an average value of -2.15‰.

The $\delta^{34}\text{S}\%$ values of sulphide minerals differ greatly among the three deposits: From south to north, the $\delta^{34}\text{S}\%$ values shift from positive to negative, and the value range of $\delta^{34}\text{S}\%$ decreases from Bake to Woxi (Fig.2).

5.2 MEASUREMENT UNITS AND NUMBERS

5.2.1 Bake deposit

According to Table 2, the δDSMOW values in Bake gold deposit ranged from -91‰ to -112.2‰, and averaged at -101.55‰, the $\delta^{18}\text{OSMOW}$ values of quartz ranged from 15.2‰ to 17.5‰ and averaged at 16.92‰, and the $\delta^{18}\text{OSMOW}(\text{H}_2\text{O})$ values of ore-forming fluids ranged from 2.14‰~4.44‰ and averaged at 3.86‰.

5.2.2 Zhazixi deposit

The δDSMOW values in Zhazixi Sb-Au deposit belonged to the interval of -49‰~-78‰, with an average value of -61.6‰, the $\delta^{18}\text{OSMOW}$ values of quartz belonged to the interval of 15.2‰~18.2‰, with an average value of 17.54‰,

TABLE 2: HYDROGEN AND OXYGEN ISOTOPES IN THE THREE DEPOSITS

Deposit	Sample serial no.	Simple mineral	$\delta D_{V-SMOW}\text{‰}$	$\delta^{18}O_{V-SMOW}\text{‰}$	$\delta^{18}O_{SMOW}(H_2O)\text{‰}$	Data sources
Bake	BK01	Quartz	-91	15.2	2.14	This study
	BK02	Quartz	-97.1	17.5	4.44	
	BK03	Quartz	-99.8	17.3	4.24	
	BK04	Quartz	-100.2	16.9	3.84	
	BK05	Quartz	-109	17.2	4.14	
	BK06	Quartz	-112.2	17.4	4.34	
Zhazixi	ZZX01	Quartz	-68	17.9	6.2	
	ZZX02	Quartz	-57	19.1	7.4	
	ZZX03	Quartz	-49	15.2	3.5	
	ZZX04	Quartz	-56	17.3	5.6	
	ZZX05	Quartz	-78	18.2	6.5	
Woxi	WX01	Quartz	-54.99	26.1	15.02	He, 1996[10]
	WX02	Quartz	-58.35	16.3	5.22	
	WX03	Quartz	-85.92	18.3	7.22	
	WX04	Quartz	-64	16.5	5.42	
	WX05	Quartz	-81	17.4	6.32	
	WX06	Quartz	-69	15.7	4.62	
	WX07	Quartz	-64	15.3	4.22	
	WX08	Quartz	-64	16.5	5.42	
	WX09	Quartz	-64	18.2	7.12	
	WX10	Quartz	-118	17.8	6.72	
	WX11	Quartz	-69	15.7	4.62	
	WX12	Quartz	-81	17.4	6.32	

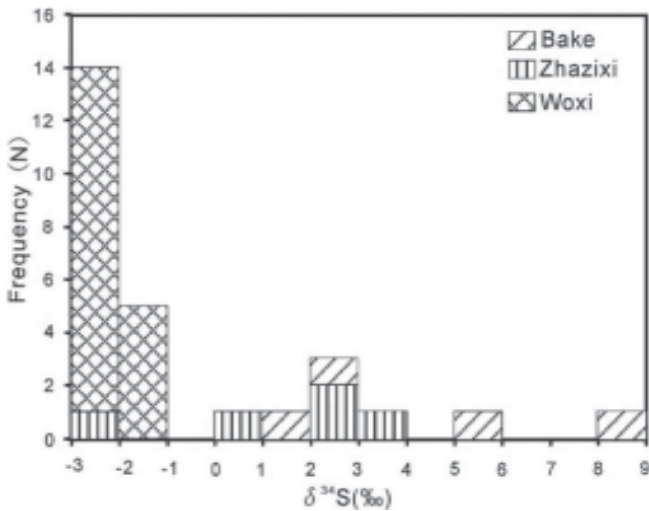


Fig.2 Bar graph of $\delta^{34}S$ of orebodies in the three deposits

and the $\delta^{18}OSMOW(H_2O)$ values belonged to the interval of 3.5‰~7.4‰, with an average value of 5.84‰.

5.2.3 Woxi deposit

11 of the 12 $\delta DSMOW$ samples had $\delta DSMOW$ values between -85.92‰ and -54.99‰, with an average value of -72.77‰. The 12th sample had an anomalous $\delta DSMOW$ of -

118‰ and was excluded from the previous calculations. The $\delta^{18}OSMOW$ values of quartz fell within 15.3‰~26.1‰, with an average value of 17.6‰, while the $\delta^{18}OSMOW(H_2O)$ values fell within 4.22‰~15.02‰, with an average value of 6.52‰ (Table 2).

5.3 LEAD ISOTOPES

For the 15 samples of simple stibnite and pyrite from the main orebody in each of the 3 deposits, the ratios of $^{208}Pb/^{204}Pb$, $^{207}Pb/^{204}Pb$ and $^{206}Pb/^{204}Pb$ were determined as follows: 37.562~37.646, 15.537~15.562 and 17.331~17.388 in Bake gold deposit; 38.167~38.928, 15.616~15.674 and 18.079~18.815 in Zhazixi Sb-Au deposit, and 37.923~39.088, 15.567~15.754 and 17.678~20.004 in Woxi Au-Sb-W deposit (Table 3).

Fig.3 shows the covariation diagram of $^{206}Pb/^{204}Pb \sim ^{207}Pb/^{204}Pb$ and $^{206}Pb/^{204}Pb \sim ^{208}Pb/^{204}Pb$ lead isotopes ratios. In the figure, Bake gold deposit fall on the area of the lower crust, Zhazixi Sb-Au deposit and Woxi Au-Sb-W deposit fall on the area of the lower crust and the area of the orogenic belt. Similar results are found in the tectonic model diagram (Fig.4) of $^{206}Pb/^{204}Pb \sim ^{207}Pb/^{204}Pb$ and $^{206}Pb/^{204}Pb \sim ^{208}Pb/^{204}Pb$ ratios, that is, the placement between orogenic belt and lower crust and between orogenic belt and upper crust.

TABLE 3: LEAD ISOTOPES IN THE THREE DEPOSITS

Mining area	Sample no.	Simple mineral	$^{206}\text{Pb}/^{204}\text{Pb}$	$^{207}\text{Pb}/^{204}\text{Pb}$	$^{208}\text{Pb}/^{204}\text{Pb}$	t(Ma)	Data sources
Bake	BK01	Galenite	17.368	15.541	37.588	840	Chen., 2015[7]
	BK02	Galenite	17.388	15.562	37.646	848	
	BK03	Galenite	17.331	15.537	37.562	861	
Zhazixi	ZZX01	Stibnite	18.575	15.619	38.753	70	This study
	ZZX02	Stibnite	18.079	15.624	38.591	434	
	ZZX03	Stibnite	18.157	15.625	38.167	380	
	ZZX04	Stibnite	18.815	15.674	38.928	-35	
	ZZX05	Stibnite	18.186	15.616	38.324	349	
Woxi	WX01	Pyrite	18.124	15.754	38.554	550	Peng et al., 2006[11]
	WX02	Pyrite	17.887	15.603	37.923	545	
	WX03	Pyrite	18.188	15.628	38.345	361	
	WX04	Tungstite	18.213	15.601	38.55	311	
	WX05	Tungstite	20.004	15.686	39.088	-938	
	WX06	Tungstite	18.115	15.610	38.576	392	
	WX07	Tungstite	17.678	15.567	38.496	652	

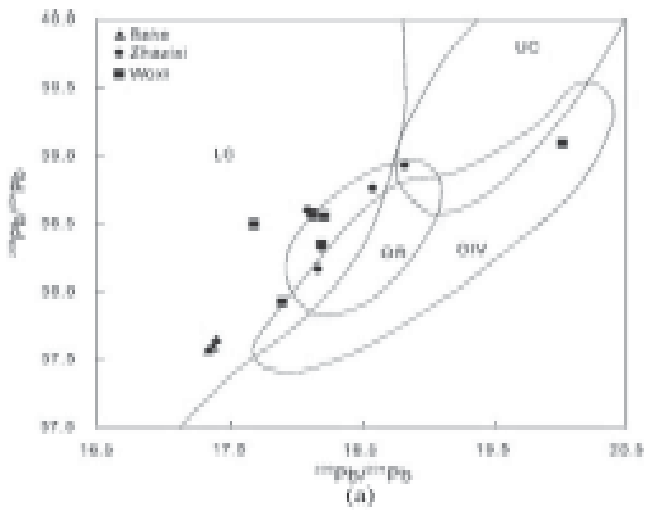


Fig.3 Covariation diagram of $^{206}\text{Pb}/^{204}\text{Pb}$ ~ $^{207}\text{Pb}/^{204}\text{Pb}$ and $^{206}\text{Pb}/^{204}\text{Pb}$ ~ $^{208}\text{Pb}/^{204}\text{Pb}$ in the three deposits
UC-upper crust; LC-lower crust; OR- orogenesis belt; OIV-mantle

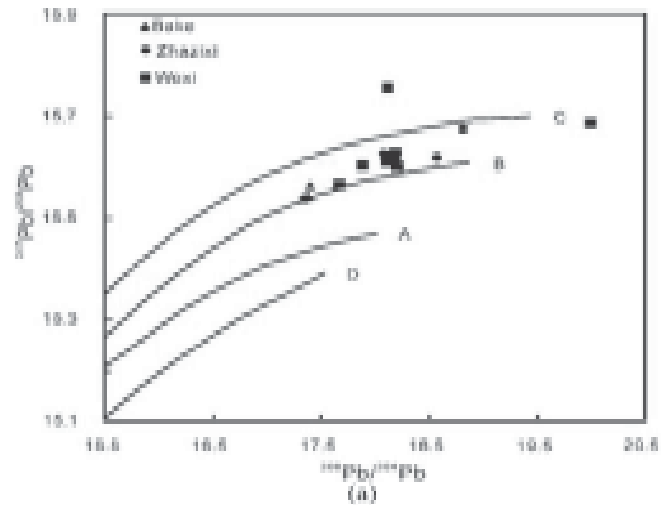


Fig.4 Tectonic model diagram of $^{206}\text{Pb}/^{204}\text{Pb}$ ~ $^{207}\text{Pb}/^{204}\text{Pb}$ and $^{206}\text{Pb}/^{204}\text{Pb}$ ~ $^{208}\text{Pb}/^{204}\text{Pb}$ in the three deposits
A-mantle; B- orogenesis belt; C-upper crust; D-lower crust

6. Discussion

6.1 FEATURES OF GOLD-BEARING STRATA AND THEIR MINERALIZATION SIGNIFICANCE

In Xuefeng belt, the gold, Au-Sb and Au-Sb-W deposits are clearly influenced by stratum features. More than 80% of gold mines, antimony mines, Au-Sb mines and Au-Sb-W mines are distributed in Neoproterozoic metamorphic rocks, siltite, and argillite in Wuqiangxi formation and Madiyi formation, Banxi Group on both sides of the local faults. The distribution pattern reflects that the two formations were connected with gold mineralization in the belt.

Based on 490 samples from Banxi Group, Yu et al. [12] obtained the average Au concentration (2.93ppb). He [10] examined unaltered rocks in Wuqiangxi and Madiyi formations, Banxi Group in Woxi Au-Sb deposit, and concluded that the Au concentration is 5.146ppb in Madiyi formation and 5.215ppb in the Wuqiangxi formation. All of these values surpass the concentrations in the upper crust (1.8ppb) [13]. Ma et al. [14] investigated 4 long geochemical sections of unaltered rocks in Madiyi formation, Banxi Group, and put the Sb background value at 1.0ppm and the average Sb content of two lithologic members at 7.4ppm and 25ppm, respectively. The results far exceed the concentrations in the upper crust (0.2ppm) [13]. Therefore, Banxi Group acts as a potential source of mineralization materials for Au and Sb deposits. Similarly, the massive amount of pyrite across Banxi Group stratum signifies that the belt boasts lots of sulphide rich in organic carbon (0.1%~4%) [10], which favours the migration of enrichment of Au and Sb.

6.2 TECTONIC EVOLUTION AND ITS CONTRIBUTION TO MINERALIZATION

Xuefeng belt was shaped by several tectonic events, such as Xuefeng period, the early Paleozoic, the Indo-Chinese epoch, the Jurassic-Cretaceous epoch and so on. Different tectonic events have different implications on the mineral deposits in the belt, and even a tectonic event still have different implications on the mineral deposits in different area of the belt [15].

Similar to the collision between the Yangtze plate and the North China-Qinling-Dabieshan complex plate, Xuefeng Mountains also underwent an early Paleozoic collision [16], whose left shearing movement created a series of NE and N-NE shear faults [17]. At that time, the whole Xuefeng belt was undergoing inland orogeny, shearing and sliding, together with some weak magmatic activity. Only a few areas were intruded by a few basic and ultra-basic rocks of limited areal extent. Hence, gold was not accumulated in large quantities at that time. Moreover, research on strontium (Sr) isotopes [18] shows that the igneous gangue rocks have nothing to do with the mineralization of gold deposit. According to geomagnetic surveys in the southern part of the belt [15], there is a uniform subsurface with no concealed igneous rock body at depth. On this basis, it is deduced that the mineralization process in this period was primarily driven by

tectonic stresses, and the raw materials came from Banxi Group strata.

The key magmato-thermal events in South China happened in Indosinian movements during Jurassic-Cretaceous period. In these periods, Xuefeng belt was affected by largescale intrusion of primarily intermediate-acid magmatite and the associated thermal activities. The mineralization occurred at widely different intensities across Xuefeng belt, due to the various crustal movements at different places in the belt. For instance, the southern parts were uplifted and depressed at the same time, while the middle and northern parts were under strong magmatic activities. These activities resulted in a plurality of intermediate-acid, large magmatic bodies formed with high concentrations of tungsten, lead, zinc and sulphide. Typical examples include Zhonghuashan, Chongyangpin, Wawutang, Baimashan, and Dashenshan and Weishan granite [19].

Therefore, it is concluded that the intermediate-acid, large magmatic bodies are potential sources of raw materials for the mineralization of tungsten deposits. As shown in Fig.1, the mineralization of gold-bearing polymetallic deposits in the middle and northern parts occurred at the same or similar times with the diagenesis of magmatite. This further proves the correlation between magmatite emplacement and regional mineralization. In addition, the sulphide content is higher in the middle and northern parts than in the southern part. Thus, the ore mineral combinations shifted from simple gold ore deposits to high-temperature polymetallic deposits like Au-Sb, Au-Sb-W, and Sb-W, which are all consistent with mineralization in association with magmatite and related thermal fluids.

More evidence for the association between magmatite and related thermal fluids can be found by examining more exotic ores containing As, Sb and W. Probing into these elements, Wall et al. [20] found that igneous thermal fluids have a strong ability to move Au and Sb and also a great impact on the enrichment of gold deposits in folded strata in later periods.

6.3 SOURCES OF MINERALIZATION MATERIALS

According to Ohmoto et al. [21], the sulphide in thermal fluid mainly exists in the form of hydrogen sulfide (HS-) and S²⁻ under reducing conditions with a low oxygen fugacity, and the $\delta^{34}\text{S}$ values of precipitating sulphide is close to the $\delta^{34}\text{S}$ of the fluid; in an oxidizing environment with a high oxygen fugacity, however, H₂S changes into SO₂ and sulphide precipitation occurs, leading to the removal of ³⁴S; in this case, the $\delta^{34}\text{S}$ sulphide in the residual fluid to a level below the $\delta^{34}\text{S}$.

The sulphides in Bake Au deposit, Zhazixi Sb-Au deposit, and Woxi Au-Sb-W deposit are mainly arsenopyrite, pyrite, and stibnite with S²⁻ existing in predictable patterns. Moreover, the surrounding rocks contain no mineral formed under oxidizing conditions, but boast a wealth of pyrite. This

means the belt was mineralized in a reducing environment. Therefore, the $\delta^{34}\text{S}$ values of sulphide in the minerals are equivalent to the $\delta^{34}\text{S}_{\Sigma}$ values of the whole fluid system at the time of deposition.

Since the region was not much affected by metamorphism, the uniformity of $\delta^{34}\text{S}_{\text{‰}}$ values in Woxi Au-Sb-W deposit cannot be the result of metamorphic alteration. Instead, the $\delta^{34}\text{S}$ values of every deposit in Xuefeng Belt must reflect the original sulphide sources, for mineral features always demonstrate the initial sulphide sources.

From south to north, the $\delta^{34}\text{S}_{\text{‰}}$ values of sulphide in orebodies differ remarkably among the three deposits. In Bake gold deposit, the $\delta^{34}\text{S}_{\text{‰}}$ value ranges between 1.6‰ and 8.95‰, which fall within the range of metamorphic rocks ($\delta^{34}\text{S}=-20\text{‰}\sim 20\text{‰}$) or sedimentary rocks ($\delta^{34}\text{S}=-40\text{‰}\sim 50\text{‰}$) according to previous research [22].

The graph of sulphide isotopes compositions (Fig.2) show that sulphide isotopes of Bake gold deposit are quite different from the magmatic sulphide of Jurassic-Cretaceous Baoshan granodiorite and the Jurassic-Cretaceous Ziyunshan granite formed in Indosinian movements. The latter two rocks are found in the vicinity of the belt. However, the sulphide isotopes are consistent with the sulphide in the local strata. The results further evidence that the mineralization materials of Bake gold deposit are originated in mineral-rich strata.

The $\delta^{34}\text{S}_{\text{‰}}$ values of Zhazixi Sb-Au deposit basically stabilize at 0‰, while those of Woxi Au-Sb-W varies in -2.8‰~-1.5‰, indicating both deposits have similar ($0\pm 3\text{‰}$) $\delta^{34}\text{S}$ values to the sulphide from deep magmatite and deep mantle sources [23]. According to the sulphide isotopes composition diagram (Fig.5), the $\delta^{34}\text{S}$ values of Zhazixi and Woxi deposits are similar to magmatic sulphide but entirely different from the sulphide of the surrounding Banxi and Lengjiaxi Group rocks. Through the above analysis, it is learned that the sulphide in minerals of Zhazixi and Woxi deposits mainly came from the magmatic rock mass.

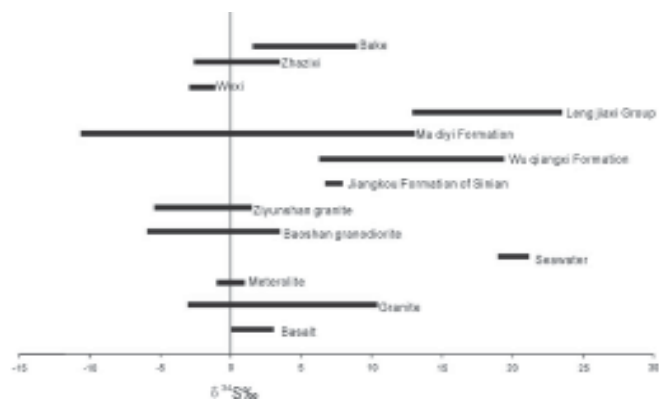


Fig.5 Composition of sulphide isotopes in the three deposits Baoshan granodiorite from Bao et al., 2014[24]; Ziyunshan granite from Zhang et al., 2015[25]; Lengjiaxi Group, Madiyi Formation and Wuqiangxi Formation from Gu et al., 2004[9]; Jiangkou Formation of Sinian from Wei., 1993[26]

Lead isotopes have been universally employed as tracers for sources of ions in metal minerals[27,28]. The $^{208}\text{Pb}/^{204}\text{Pb}$, $^{207}\text{Pb}/^{204}\text{Pb}$ and $^{206}\text{Pb}/^{204}\text{Pb}$ ion ratio values are similar throughout Zhazixi deposit and the Woxi deposit, indicating that the two deposits have similar lead sources. In other words, the two deposits bear high resemblances in terms of base foundations and tectonic background. By contrast, Bake gold deposit is considerably different from its northern counterparts in lead sources. The lead model age calculations show that Zhazixi deposit is between -35Ma and 434Ma, and Woxi deposit is between -938Ma and 652Ma. The broad range manifests that the lead in the two deposits originate from mixed sources, while the narrow range (840~861Ma) of lead isotope ages of Bake deposit is an evidence of uniform lead sources and simple tectonic depositional pathways. These results are proved accurate by their consistency with hydrogen and oxygen isotopes.

As can be seen from the diagrams of lead isotopes (Figs.3 and 4), the samples of Bake gold deposit are concentrated within or near the crust, indicating that the lead was provided by a single source. On the contrary, the samples of Zhazixi Sb-Au deposit and Woxi Au-Sb-W deposit are relatively scattered, revealing that the lead came from a mixture of sources. As a result, the lead mineralization materials in Bake deposit were derived from the crust, and those in the other two deposits were sourced from both the crust and mantle.

6.4 SOURCES OF MINERALIZATION FLUIDS

Hydrogen and oxygen are popular tracers of mineralization fluid sources in thermal fluid deposits [22,29,30]. After exploring the hydrogen and oxygen isotopes in the three

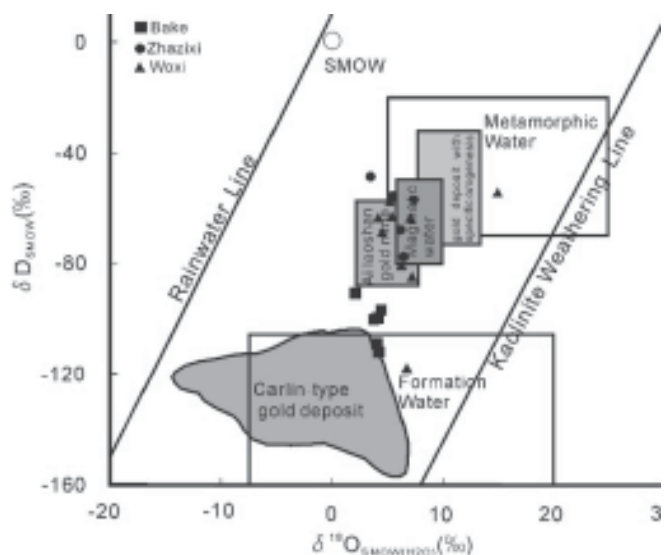


Fig.6 Diagram of $\delta\text{D}_{\text{SMOW}}-\delta^{18}\text{O}_{\text{SMOW}}(\text{H}_2\text{O})$ isotopes compositions in granite vein fluid of the three deposits

Carlin-type gold deposit from Field et al., 1985[31]; Formation water from Slieppard., 1986[32]; Ailaoshan gold mine from Sun et al., 2009[33]; Gold deposit with specific orogenesis from Goldfarb et al., 2004[34]

deposits, the author discovered that the H and O isotopes are similar to S and Pb isotopes in Bake deposit, but different from the latter in the other two deposits.

Fig.6 is the $\delta D_{SMOW}-\delta^{18}O_{SMOW}(H_2O)$ isotopes diagram. It can be seen that the samples of Bake deposit, similar to Carlin-type gold deposits, are plotted in close proximity with formation water, but far from metamorphic and magmatic water. Thus, the deposit's mineralization fluids are the mixture of formation water with a small quantity of meteoric water. The samples of Zhazixi and Woxi deposits are plotted as metamorphic water, magmatic water, or a structurally deformed area containing both types of water. The pattern is similar to that of gold deposits formed in an orogenic environment (e.g. Ailaoshan Mountains in Yunnan Province). This means the hydrogen and oxygen isotopes in Zhazixi and Woxi deposits originate from the same fluid sources: metamorphic water and magmatic water.

7. Conclusions

Through hydrogen (H)-oxygen (O)-sulphur (S)-lead (Pb) isotope analysis, the sources of mineralization materials and mineralization fluids at the three typical deposits in Xuefeng belt are identified as follows:

- (1) Sulphur and lead isotopes in minerals have different sources in southern, middle, and northern parts of the belt. Sulphur and lead in the southern deposit mainly came from the crust, while those in the middle and northern deposits primarily originate from deeper places in the earth.
- (2) The thermal fluids associated with mineralization have different sources in southern, middle, and northern parts of the belt. Most of the fluids derived from formation water and meteoric water in the south, and from magmatic water and metamorphic water in the middle and northern parts.
- (3) Xuefeng belt experienced two distinct mineralization periods: the early Paleozoic period and the Jurassic-Cretaceous period. The metallogenic dynamics in the early Paleozoic period was mainly shear-tectonic movement, but the metallogenic dynamics in the Indosinian movements during the latter period came from magmatic movement, which reformed the mineralization with sulfur-rich magmatic hydrothermal fluids.

Acknowledgment

This paper is made possible by the generous support from the National Natural Foundation of Science of China (Grant No.: 41672082), Hao Li Fuchu and two anonymous reviewers.

References

1. Su, K. M. and Zeng, Y. (2007): "Gold deposit type and its distribution characteristic in Snowberg Arc Structure Belt," *Gold*, Vol. 28, p. 19-22, 2007.
2. Dobrota, D. and Petrescu, V. (2015): "Modelling of the

heat transfer in the process of joining by vulcanisation of conveyor belts," *Academic Journal of Manufacturing Engineering*, Vol.13, No.2, pp. 48-53, 2015.

3. Li, F. K., Deng, A.Z., Rong, X., Chen, K. and Li, H. N. (2017): "Study on the preparation of column-cell and its influence on mechanical properties by deep drawing," *Journal of Manufacturing Engineering*, Vol.15, No.3, pp.119-128, 2017.
4. Fan, J. W., Liu, Y., Liu, L. L. and Yang, S. R. (2017): "Hydrodynamics of residual oil droplet displaced by polymer solution in micro-channels of lipophilic rocks," *International Journal of Heat and Technology*, Vol. 35, No. 1, pp. 611-618, 2017.
5. Rajput, G. R., Patil, V. S. and Krishna, P. J. S. V. R. (2017): "Hydromagneticbioconvection flow in the region of stagnation-point flow and heat transfer in non-Newtonian nanofluid past a moving surface with suction: similarity analysis," *International Journal of Heat and Technology*, Vol. 35, No. 1, pp. 25-31, 2017.
6. Y, D. L. (1997): "A study on the geological and geochemical characteristics of bake gold deposit, east Guizhou," *Earth and Environment*, pp. 12-17, 1997.
7. Chen, Y. (2015): "Features and structures of gold metallogenic system of the Tianzhu-Jinping Areas," Southeastern Guizhou, China: Wuhan, China University of Geosciences, p.54-56, 2015.
8. Lai, X. Y. and He, M. Q. (2010): "Geochemical study of fluid inclusions of bake gold deposit in Jinping county of guizhou province," *Journal of Guizhou University (Natural Sciences)*, Vol. 27, p. 33-36, 2010.
9. Gu, X. X., Liu, J. M., Oskar, S., Franz, V. and Zheng, M. H. (2004): "Syngeneticcoricin of the Woxi W Sb Au deposit in Hunan: Evidence from trace elements and sulfur isotopes," *Chinese Journal of Geology*, Vol. 39, p. 424-439, 2004.
10. He, G. X. (1996): "Geological features and ore-hunting prospects of Woxi gold deposit in western Hunan," *Gold Geology*, Vol.2, p. 45-49, 1996.
11. Peng, B., Robert, F. and Tu, X. L. (2006): "Nd-Sr-Pb isotopic geochemistry of scheelite from the Woxi W-Sb-Au deposit, Western Hunan: Implications for sources and evolution of ore-forming fluids," *Acta Geologica Sinica*, Vol.80, p. 561-570, 2006.
12. Yu, D. L., Zhou, D. Z., Zhang, R. R., Ye, D. Y., Rao, Z. P. and Chen, Q. N. (1999): "A study on the gold-bearing potential of the strata in Hunan and east Guizhou," *Acta Mineralogical Sinica*, Vol. 19, p. 362-369, 1999.
13. Taylor, S. R. and McLennan, S. M. (1995): "The geochemical evolution of the continental crust," *Reviews of Geophysics*, Vol. 33, p. 241-265, 1995.

14. Ma, D. S. and Bernd, L. (2000): "The Multi-peak Structure of the stibium content in Ma Diyi Formation of West Hunan Gold deposit and its region: Application of the cumulative probability ruled form for gold deposit genesis and exploration," *Bulletin of Mineralogy, Petrology and Geochemistry*, Vol. 19, p. 218-220, 2000.
15. Peng, J. T. (1999): "Gold mineralization and its evolution in the Xuefeng district, Hunan," *Geotectonica et Metallogenia*, Vol. 23, p. 144-151, 1999.
16. Dai, C. G. (2010): "Geologic character and tectonic evolution of the east Guizhou and its adjacent region," Beijing, China University of Geosciences, p. 1-127, 2010.
17. Qiu, Y. X., Ma, W. P., Fan, X. L., Zhang, Y. C., Deng, J. R., Xia, L. H. and Zhang, X. L. (1996): "Tectonic nature and tectonic evolution of the Xuefeng Oldland in the Early Paleozoic stage," *Regional Geology of China*, Vol.2, p. 150-160, 1996.
18. Wang, X. Z., Liang, H. Y., Shan, Q., Cheng, J. P. and Xia, P. (1999): "Metallogenic age of the Jinshan gold deposit and early Paleozoic gold mineralization in South China," *Geological Review*, Vol. 45, p. 19-25, 1999.
19. Su, K. M., Lu, S. J., Kong, L. B., Yang, F. Q. and Xiang, J. F. (2016): "Geological characteristics, metallogenetic regularity and model of quartz vein type tungsten deposits in Chongyangping, Hunan Province," *Mineral Deposits*, Vol. 35, p. 902-912, 2016.
20. Wall, V. J., Yantzen, V. and Graupner, T. (2004): "Muruntau. Uzbekistan Report on CERCAMS Research Project," Spring Hill: Taylor Wall & Associate, 2004.
21. Ohmoto, H. and Rye, R. O. (1979): "Isotopes of sulfur and carbon. In: Barnes HL (ed.)," *Geochemistry of Hydrothermal Ore Deposits*: New York, John Wiley, p. 509-567, 1979.
22. Hoefs, J. (1997): "Stable isotope geochemistry," 4th Edition: Berlin Heidelberg, Springer-Verlag, p. 65-168, 1997.
23. Rollinson, H. R. (1993): "Using geochemical data: Evaluation, presentation, Interpretation," New York, John Wiley & Sons, p. 1-352, 1993.
24. Bao, T., Ye, L., Yang, Y. L. and Li, Z. L. (2014): "Characteristics of sulfur isotope geochemistry of Baoshan Cu-Mo-Pb-Zn-Ag polymetallic deposit, Hunan Province and its geological significance," *Acta Mineralogica Sinica*, Vol. 34, p. 261-266, 2014.
25. Zhang, L. J., Shao, Y. J., Lai, J. Q., Shi, J. and Xu, Z. B. (2015): "Analysis on ore-controlling alteration rocks and structures in the Baojinshan-Jinkengchong gold deposit, Hunan province: *Mineral Exploration*," Vol. 6, p. 245-253, 2015.
26. Wei, D. F. (1993): "Source of ore-forming materials in Canziping gold deposit and the geologic study of its mechanism of formation," *Human Geology*, Vol. 12, p. 29-34, 1993.
27. Macfarlane, A. W., Marcet, P., LeHuray, A. P. and Petersen, U. (1990): "Lead isotope provinces of the Central Andes inferred from ores and crustal rocks: *Economic Geology*," Vol. 85, p. 1857-1880, 1990.
28. Chiaradia, M., Fontboté, L. and Paladines, A. (2004): "Metal sources in mineral deposits and crustal rocks of Ecuador (1°N-4°S)," A lead isotope synthesis: *Economic Geology*, Vol. 99, p. 1085-1106, 2004.
29. Zheng, Y. F. and Chen, J. F. (2000): "Stable Isotope Geochemistry," Beijing, Science Press, p.193-217, 2000.
30. Pirajno, F. (2009): "Hydrothermal processes and mineral system." Berlin, Springer, p. 1-1250, 2009.
31. Field, C. W. and Fifarek, R. H. (1985): "Light stable-isotopic systematics in the epithermal environment," *Reviews in Economic Geology*, Vol. 2, p. 99-128, 1985.
32. Slippard, S. M. F. (1986): "Characterization and isotopic variations in natural waters," *Reviews in Mineralogy*, Vol. 16, p. 165-183, 1986.
33. Sun, X. M., Zhang, Y., Xiong, D. X., Sun, W. D., Shi, G. Y., Wei, Z. and Wang, S. W. (2009): "Crust and mantle contributions to gold-forming process at the Daping deposit, Ailaoshan gold belt, Yunnan, China," *Ore Geology Reviews*, Vol. 36, p. 235-249, 2009.
34. Goldfarb, R. J., Ayuso, R., Miller, M. L., Ebert, S. W., Marsh, E. E., Petsel, S. A., Miller, L. D., Bradley, D., Johnson, C. and McClelland, W. (2004): "The late cretaceous Donlin Creek gold deposit, Southwestern Alaska," *Controls on Epizonal Ore Formation: Economic Geology*, Vol. 99, p. 643-671, 2004.

Journal of Mines, Metals & Fuels

Special issue on

CSR in the mining industry

For copies, contact :

Tel.: 0091 33 22126526 Fax: 0091 33 22126348 e-mail: bnjournals@gmail.com